ACS APPLIED MATERIALS & INTERFACES

Research Article

www.acsami.org

Simple Way to Engineer Metal–Semiconductor Interface for Enhanced Performance of Perovskite Organic Lead Iodide Solar Cells

Yuzhuan Xu,[†] Jiangjian Shi,[†] Songtao Lv,[†] Lifeng Zhu,[†] Juan Dong,[‡] Huijue Wu,[†] Yin Xiao,[‡] Yanhong Luo,[†] Shirong Wang,[‡,§] Dongmei Li,*[,†] Xianggao Li,*[,‡,§] and Qingbo Meng*[,†,§]

[†]Key Laboratory for Renewable Energy, Chinese Academy of Sciences, Beijing Key Laboratory for New Energy Materials and Devices, Institute of Physics, Chinese Academy of Sciences, Beijing, 100190, China

[‡]School of Chemical Engineering and Technology, Tianjin University, Tianjin 300072, China

[§]The Co-Innovation Center of Chemistry and Chemical Engineering of Tianjin, Tianjin 300072, China

Supporting Information

ABSTRACT: A thin wide band gap organic semiconductor *N,N,N′,N′*-tetraphenyl-benzidine layer has been introduced by spin-coating to engineer the metal–semiconductor interface in the hole-conductor-free perovskite solar cells. The average cell power conversion efficiency (PCE) has been enhanced from 5.26% to 6.26% after the modification and a highest PCE of 6.71% has been achieved. By the aid of electrochemical impedance spectroscopy and dark current analysis, it is revealed that this modification can increase interfacial resistance of $CH_3NH_3PbI_3$/Au interface and retard electron recombination process in the metal–semiconductor interface.

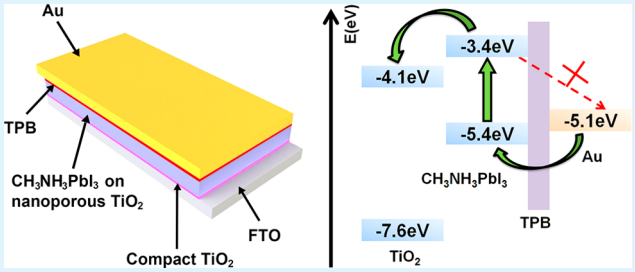

KEYWORDS: *N,N,N′,N′-tetraphenyl-benzidine (TPB), perovskite solar cell, metal–semiconductor (M–S) interface, modification*

1. INTRODUCTION

Organo-lead perovskite with balanced long-range carrier diffusion lengths[1−3] and low-cost have attracted great attention as a new class of light harvesters for solid-state hybrid solar cells in the past few years.[4] The highest power conversion efficiency (PCE) over 15% has been reported with 2,2′,7,7′-tetrakis[*N,N*-di(4-methoxyphenyl)amino]-9,9′-spirobifluorene (spiro-MeO-TAD) as a hole-transport material (HTM).[5−9] Recently, HTM-free perovskite solar cells have also been developed since the perovskite itself can be both the light harvester and hole conductor. Moreover, the structure of the HTM-free perovskite solar cells is simpler and the fabrication cost can be reduced greatly.[10−12]

In HTM-free perovskite solar cells, a Schottky contact at the metal–semiconductor (M–S) interface exists between $CH_3NH_3PbI_3$ and Au. The M-S interface has strong influence on the performance of semiconductor-based electronic devices. Constructing ohmic contact is a general way to facilitate smooth charge transportation. Heavy doping is a common method to obtain a suitable ohmic contact at the M–S interface.[13,14] However, this method does not work in this kind of perovskite solar cells because of the thermal instability of $CH_3NH_3PbI_3$.[15] Therefore it is required to develop suitable methods to modify the M–S interface under mild condition. Recently, an ultrathin Al_2O_3 insulator layer has been used to construct a metal–insulator–semiconductor back contact in HTM-free perovskite solar cells by atomic layer deposition (ALD) technology[16] in our group. An enhanced PCE from 3.30% to 5.07% was obtained. This ALD technique can provide high-quality ultrathin films on the atomic scale at relatively low temperature,[17] which is effective on M–S interface modification. However, ALD technique has the problems of strict working environment like vacuum and high cost precursors. Therefore, it is worth developing cheap and simple ways to modify the M–S interface.

N,N,N′,N′-Tetraphenyl-benzidine (TPB) is a widely used wide band gap organic semiconductor in OLEDs.[18] As shown in Figure 1, its highest occupied molecular orbital (HOMO) is lower than and lowest unoccupied molecular orbital (LUMO) is higher than those of the lead iodide perovskite $CH_3NH_3PbI_3$ (Figure 1), respectively. This means that TPB has a similar relative energy level as Al_2O_3 in the HTM-free perovskite solar cells.[16] Therefore, TPB can play the same role as Al_2O_3 in HTM-free perovskite solar cells. Moreover, TPB layer can be fabricated with solution method which will highly simplify the producing process and reduce cost. In the present work, a spin-coating process has been used to build a thin TPB layer on the surface of $CH_3NH_3PbI_3$ layer to modify the M–S interface in HTM free perovskite solar cells. The average PCE of the solar cells have been enhanced from 5.26% to 6.26% with a highest PCE of 6.71% after modification. The modification towards

Received: January 9, 2014
Accepted: April 1, 2014
Published: April 1, 2014

   dx.doi.org/10.1021/am5001773 | *ACS Appl. Mater. Interfaces* 2014, 6, 5651−5656

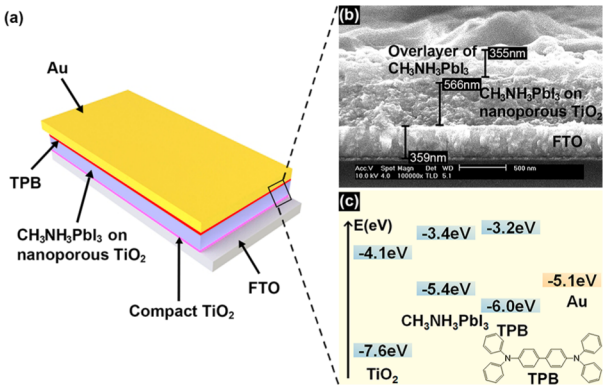

Figure 1. (a) Schematic of device architecture. (b) Cross-sectional SEM image of the device. (c) TPB chemical structure and energy level alignment of different components in organo-lead perovskite photovoltaic devices.

M−S interface was further investigated by electrochemical impedance spectroscopy (EIS).

2. EXPERIMENTAL SECTION

2.1. Materials. PbI_2 was purchased from Aldrich, and dimethylformide (DMF) was purchased from Alfar Aesar. TPB was prepared according to the procedure reported and confirmed by comparing their characterization data with the literature data.[19] CH_3NH_3I was synthesized by following the literature.[20,21] Substrates are fluorine-doped tin oxide conducting glass (FTO, Pilkington, thickness 2.2 mm, sheet resistance 14 Ω/square). Before use, FTO glass was first washed with mild detergent, rinsed with distilled water for several times and subsequently with ethanol in an ultrasonic bath, finally dried under air stream.

TPB. White solid (72 %). mp: 224−226 °C. ^{1}H NMR (500 MHz, $CDCl_3$): δ (ppm) 7.46 (d, J = 8.5 Hz, 4H), 7.29 (t, J = 7.5 Hz, 8H), 7.14 (d, J = 6.5 Hz, 12H), 7.04−7.02(m, 4H). IR (cm^{-1}, KBr): 3030, 1590, 1490, 1320, 1280, 818, 754, 698. MS (APCI) m/z 489.2 [M^+]; calcd. for $C_{36}H_{28}N_2$ 489.2.

2.2. Fabrication of the Perovskite Photovoltaic Cells with or without TPB Layer. The compact TiO_2 layers were spin-coated on the FTO and calcined at 450 °C for 30 min.[15,22] Six-hundred-nanometer-thick TiO_2 nanoporous layers (20 nm anatase TiO_2 particles) were subsequently deposited by using screen-printing technique, which were dried at 80 °C for 30 min, then sintered at 450 °C.[21] Before use, the films were immersed into 25 mM $TiCl_4$ at 70 °C for 40 min and finally sintered at 500 °C for 30 min.

$CH_3NH_3PbI_3$ layer was deposited by repeated sequential deposition method.[6,16,23,24] Firstly, 1M PbI_2 dissolved in *N*,*N*-dimethylformamide (DMF) was spin-coated onto TiO_2 film at a speed of 2000 rpm for 60 s and then heated at 100 °C for 5 min to remove DMF solvent. After it was cooled to room temperature, the film was spin coated again to get a relatively thick and smooth film, which were subsequently heated at 100 °C for 30 min. PbI_2 films were kept in 10 mg/mL CH_3NH_3I isopropanol solution for 10 min, then rinsed with isopropanol to give $CH_3NH_3PbI_3$ absorber layer. Finally, the $CH_3NH_3PbI_3/TiO_2$ films were heated at 100 °C for 30 min in air with a hotplate.

The TPB layers were then deposited by spin-coating with TPB/chlorobenzene solution (20 mg/mL and 60 mg/mL) at 3000 rpm for 30 seconds. 80 nm-thickness Au electrodes were deposited onto the prepared films by thermal evaporation (Kurt J. Lesker) at an atmospheric pressure of 10^{-7} Torr to complete the solar cells. The cells without TPB layer were fabricated by the same way except the spin-coating step of TPB.

2.3. Characterizations. The current density-voltage (J−V) characteristics of the cells were recorded on Princeton Applied Research, Model 263 under AM 1.5 100 mW/cm^2 irradiation obtained from Oriel Solar Simulator 91192. The surface morphology and composition of samples was characterized by a scanning electron microscope (SEM, FEI XL30 S-FEG). The thickness of TiO_2 layers was measured by a surface profiler (KLA-TencorP-6). Electrochemical impedance spectroscopy (EIS) measurements were performed with an IM6ex electrochemical workstation (ZAHNER) in the frequency range between 0.1 and 10^6 Hz with perturbation amplitude of 10 mV.

3. RESULTS AND DISCUSSION

3.1. Structure of $CH_3NH_3PbI_3$ Based Solar Cells. Figure 1a presents the schematic diagram of the solid-state photovoltaic devices in this work. TPB layer is used to prevent the direct contact between Au and $CH_3NH_3PbI_3$ layer. The pores of the mesoscopic TiO_2 film are infiltrated with $CH_3NH_3PbI_3$ perovskite and overlayers are observed from the cross-sectional SEM image of the nanoporous TiO_2 film (Figure1b). Surface profilometer results show that the thickness of the cells with thin TPB layer or without TPB layer is about 1.0 μm whereas the thickness of the cells with thick TPB layer is about 1.2 μm. However, it is difficult to measure the thickness of the thin TPB layer from SEM or surface profilometer directly. The energy level diagram of the perovskite solar cell with TPB layer between Au and $CH_3NH_3PbI_3$ is shown in Figure 1c. The HOMO energy level of TPB (−6.0 eV)[18] is lower than the valence band edge of $CH_3NH_3PbI_3$ (−5.4eV).[11] Therefore, a hole-transport barrier exists in this structure. In the meantime, the LUMO energy level of TPB (−3.2 eV)[18] is higher than the conduction band edge of $CH_3NH_3PbI_3$ (−3.4eV),[11] which is also an electron-transport barrier from $CH_3NH_3PbI_3$ to Au. Obviously, the TPB layer can retard both the electron and hole transport from $CH_3NH_3PbI_3$ to Au cathode, leading to two opposite effects on cell performance that retarding electron-transport enhances PCE while retarding hole-transport reduces PCE. Therefore the key is how to balance the above two effects.

3.2. Photovoltaic Performance. The J−V characteristics of the best performed perovskite solar cells without and with TPB layer under AM 1.5G irradiation of 100 mW/cm^2 are shown in Figure 2. For the cell without TPB, a highest PCE of 5.67% was achieved with short-circuit photocurrent density (J_{sc}) of 11.88 mA/cm^2, open-circuit photovoltage (V_{oc}) of 734 mV and fill factor (FF) of 0.65. When a thin TPB layer is introduced into the perovskite solar cell, the PCE was highly increased to 6.71% with J_{sc} of 14.1 mA/cm^2, V_{oc} of 786 mV, and FF of 0.61. The performance improvement in the cell with a thin layer TPB mainly lies on the increase of J_{sc} and V_{oc} compared to the cells without TPB. Statistical data of five photovoltaic devices is shown in Figure 2b and the statistical result is shown in Table 1. The result is in complete accord with conclusion by analyzing the highest cell performance. Moreover, from the average performance parameters and the small standard deviation, we infer that the enhanced performance with TPB interface modification is high reproducibility using the method reported here. Besides, the dark current is significantly suppressed when a thin TPB layer is introduced, in good agreement with the higher open-circuit voltage.[25]

To understand the function of TPB in the cell better, the cell performance of the device with thick TPB layer was also investigated. We can see that, the introduction of thick TPB layer leads to a decrease in J_{sc} and FF and a poor PCE of 4.58% as shown in Table 1 and Figure 2. As we mentioned above, to the device with thick TPB layer, the TPB mainly as the hole conductor does not match the band alignment in the band structure (Figure 1c), thus leading to unsatisfied cell performance.

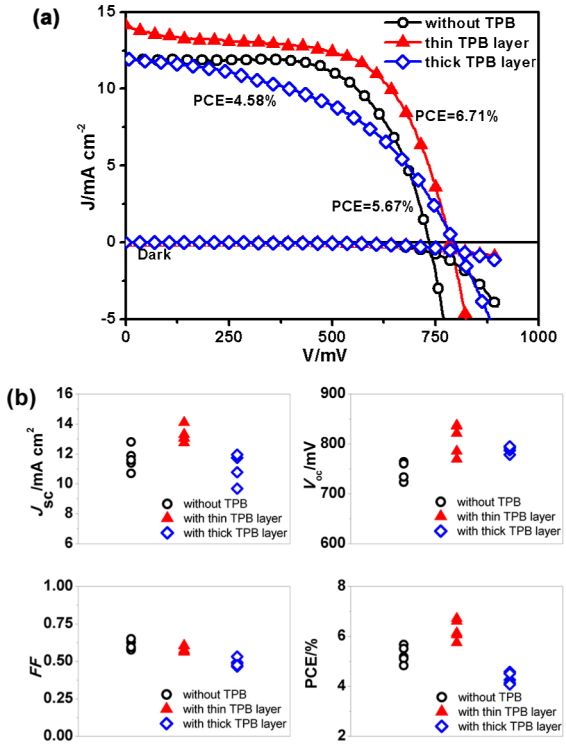

Figure 2. (a) $J-V$ curves obtained from the best perovskite solar cells without and with the TPB layer under light irradiation and in the dark. (b) Photovoltaic parameters of fifteen devices in three condition (every condition has five devices) measured under 100 mW/cm^2 simulated AM 1.5G irradiation

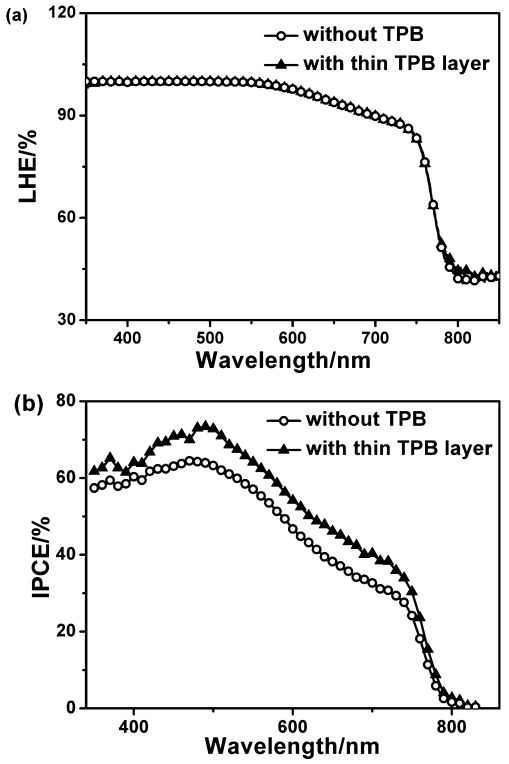

Figure 3. (a) UV–vis light-harvesting efficiency (LHE) spectra of $CH_3NH_3PbI_3/TiO_2$ films and (b) IPCE spectra of the $CH_3NH_3PbI_3$-based solar cells without and with thin TPB layers.

Table 1. Statistical IV Data of Perovskite Solar Cells with Different Modifications in the M–S Interface

	J_{sc} (mA cm^2)[a]	V_{oc} (mV)[a]	FF[a]	PCE (%)[a]
without TPB layer	11.68 ± 0.76	743 ± 18	0.61 ± 0.03	5.26 ± 0.33
thin TPB layer (20 mg/mL)	13.26 ± 0.51	810 ± 31	0.58 ± 0.02	6.26 ± 0.40
thick TPB layer (60 mg/mL)	11.18 ± 0.96	789 ± 7	0.49 ± 0.03	4.31 ± 0.22

[a]Mean ± standard deviation of each data point with five devices.

It should be pointed out that the introduction of a thin TPB layer does not have significant influence on the light absorption of cells (see in Figure 3a). Incident-photon-to-current conversion efficiency (IPCE) measurement is valuable to characterize the photocurrent in thin film solar cells.[25−27] It is found that the device with a thin TPB layer presents relatively higher IPCE values in the whole measured wavelength than that without TPB, as shown in Figure 3b. This improvement of IPCE is mainly attributed to the enhanced internal quantum efficiency (IQE), which is related to the improvement of the photogenerated carriers transport and collection properties in perovskite, in agreement with the decrease of dark current.

3.3. Electrochemical Impedance Spectra. To explore the influence of the TPB layers on the charge recombination, the cells with the structures of $TiO_2/CH_3NH_3PbI_3/Au$, $TiO_2/CH_3NH_3PbI_3$/thin TPB layer/Au, and $TiO_2/CH_3NH_3PbI_3$/thick TPB layer/Au are analyzed by EIS.[14,28−30] Figure 4 presents the Nyquist plots obtained for the above-mentioned devices in the dark at various bias voltages. The spectra pattern in Figure 4a and Figure 4b is composed by one RC arc and a low frequency feature in the whole measured frequency range. The high-frequency part of the spectra may contain information of transport and series resistance elements, as well as dielectric contributions.[31] Therefore, a similar transmission line model employed for dye solar cells[27] is simplified since transport resistance in TiO_2 could be negligible at high bias voltage as Figure 5a shows.[32] R_S is the series resistance of the device. R_1 and C_1 of CPE_1 are the interface resistance and capacitance of the $TiO_2/CH_3NH_3PbI_3$ interface in the low frequency range. R_{ct} is the interfacial charge-transfer resistance (or recombination resistance) of the $CH_3NH_3PbI_3$/Au interface. C_μ of CPE_μ is its chemical capacitance. In the Nyquist plots, the main arcs in Figure 4a and Figure 4b is caused by $CH_3NH_3PbI_3$/Au interface in high frequency region, which consists of the recombination resistance (R_{ct}) and the chemical capacitance of the interface (C_μ).[14,33] However, the spectra pattern of the device with thick TPB layer is significantly different, as shown in Figure 4c, which one oblate arc can be subdivided into two RC arcs. It is supposed that, to the system with thick TPB layer, two new interfaces of the $CH_3NH_3PbI_3$/TPB and the TPB/Au interfaces have to be considered. Therefore, the equivalent circuit in Figure 5a is not suitable for fitting the spectra pattern of the device with thick TPB layer, and the fitting results in detail are given in the Supporting Information, for the fitting interface resistances are not comparable with the R_{ct} in Figure 5b.

The fitting results are shown in Figure 5. By introducing a TPB layer, the R_{ct} increases about three times compared to M–S back contact (Figure 5b). And this enhancement of R_{ct} is supposed to favor the reduction of dark current and lead to the improvement in V_{oc}, as shown in Figure 6. In another word, the

dx.doi.org/10.1021/am5001773 | ACS Appl. Mater. Interfaces 2014, 6, 5651−5656

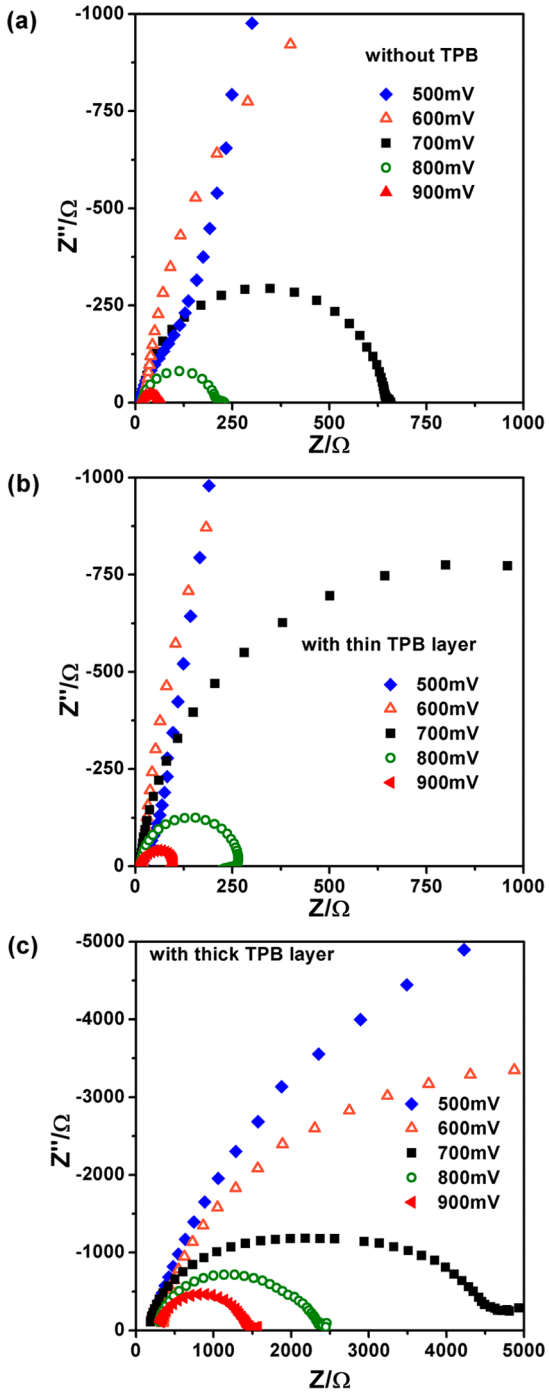

Figure 4. Nyquist plots of perovskite solar cells under dark with different modifications in the M−S interface at various bias voltages. (a) Perovskite cell without TPB layer. (b) Perovskite cell with thin TPB layer. (c) Perovskite cell with thick TPB layer.

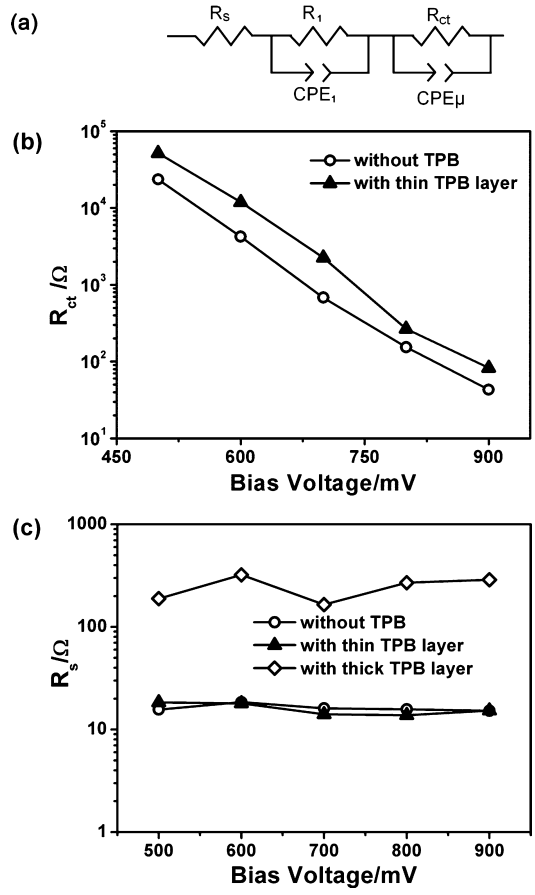

Figure 5. (a) Equivalent circuit employed to fit the Nyquist plots. (b) Fitted charge transport resistance of $CH_3NH_3PbI_3$/Au interface and (c) series resistance of perovskite solar cells with different modifications in the M-S interface at various bias voltages.

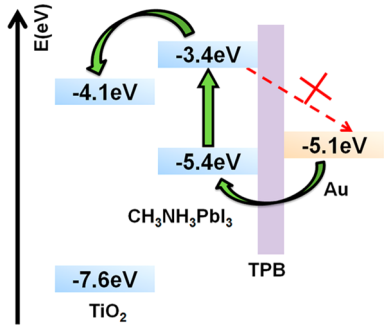

Figure 6. Schematic diagram of the electron transfer and recombination at the M−S interface in perovskite-based solar cells

existence of TPB layer can well suppress the electron recombination, which is in good accordance with the result of dark current measurement. As previously reported,[34] FF is determined by many parameters, which interplay with each other intricately. Although the modification suppresses the carrier recombination, no obvious change in the FF is observed when the thin TPB layer is introduced, which is in agreement with the similar R_s. However, when the TPB layer is getting thicker, the FF decreases since the R_s increases over ten times, as shown in Figure 5c. At this point, the charge carrier block function of TPB layer has been proved. Furthermore, both of the electron-transport block function and the hole-transport block function are well balanced by controlling the thickness of TPB layer since the R_{ct} is increased whereas R_s is unchanged after modification with thin TPB layer. However, as for the hole-transport mechanism, we cannot give a credible explanation at present. Nevertheless, there is a similar bathocuproine (BCP) layer acting as an exciton-blocking layer in planar organic solar cells, which shows a similar influence on $J-V$ performance.[35] It may be a reference to understand this work; however, further investigation is still needed in the future.

dx.doi.org/10.1021/am5001773 | ACS Appl. Mater. Interfaces 2014, 6, 5651−5656

4. CONCLUSION

In conclusion, we have developed a simple solution process to engineer the M−S interface in perovskite-based solar cells. The average PCE has been enhanced from 5.26% to 6.26% after modification and a highest efficiency of 6.71% has been achieved for perovskite-based solar cells with a thin TPB layer between $CH_3NH_3PbI_3$ and Au. Moreover, by the aid of EIS and dark current analysis, it is found that the existence of a thin TPB layer can well inhibit charge recombination at the back Schottky contact in perovskite-based solar cells. We believe that this work may help to understand the recombination processes in this kind of perovskite solar cells.

■ ASSOCIATED CONTENT

Supporting Information

Analysis of the Nyquist plots of the device with thick TPB layer, which contains equivalent circuit, fitting results, and discussion. This information is available free of charge via the internet at http://pubs.acs.org/.

■ AUTHOR INFORMATION

Corresponding Authors

*E-mail: dmli@iphy.ac.cn
*E-mail: lixianggao@tju.edu.cn.
*E-mail: qbmeng@iphy.ac.cn

Notes

The authors declare no competing financial interest.

■ ACKNOWLEDGMENTS

The authors would like to thank the financial support from National Key Basic Research Program (973 project, No. 2012CB932903), the NSFC (Nos. 21173260 and 91233202), Beijing Science and Technology Committee (Z131100006013003). The authors also thank Mr. Yueyong Yang, Mr. Junyan Xiao, Ms. Dongfeng Lin for their helpful discussions.

■ REFERENCES

(1) Xing, G.; Mathews, N.; Sun, S.; Lim, S. S.; Lam, Y. M.; Grätzel, M.; Mhaisalkar, S.; Sum, T. C. Long-Range Balanced Electron- and Hole-Transport Lengths in Organic−Inorganic $CH_3NH_3PbI_3$. *Science* **2013**, *342*, 344−347.

(2) Stranks, S. D.; Eperon, G. E.; Grancini, G.; Menelaou, C.; Alcocer, M. J. P.; Leijtens, T.; Herz, L. M.; Petrozza, A.; Snaith, H. J. Electron−Hole Diffusion Lengths Exceeding 1 Micrometer in an Organometal Trihalide Perovskite Absorber. *Science* **2013**, *342*, 341−344.

(3) Edri, E.; Kirmayer, S.; Cahen, D.; Hodes, G. High Open-Circuit Voltage Solar Cells Based on Organic−Inorganic Lead Bromide Perovskite. *J. Phys. Chem. Lett.* **2013**, *4*, 897−902.

(4) Snaith, H. J. Perovskites: The Emergence of a New Era for Low-Cost, High-Efficiency Solar Cells. *J. Phys. Chem. Lett.* **2013**, *4*, 3623−3630.

(5) Liu, M.; Johnston, M. B.; Snaith, H. J. Efficient Planar Heterojunction Perovskite Solar Cells by Vapour Deposition. *Nature* **2013**, *501*, 395−398.

(6) Burschka, J.; Pellet, N.; Moon, S. J.; Humphry-Baker, R.; Gao, P.; Nazeeruddin, M. K.; Grätzel, M. Sequential Deposition as a Route to High-Performance Perovskite-Sensitized Solar Cells. *Nature* **2013**, *499*, 316−319.

(7) Liu, D.; Kelly, T. L. Tunable Lifetime Multiplexing Using Luminescent Nanocrystals. *Nat. Photonics* **2014**, *8*, 32−36.

(8) Wang, J. T.-W.; Ball, J. M.; Barea, E. M.; Abate, A.; Alexander-Webber, J. A.; Huang, J.; Saliba, M.; Mora-Sero, I.; Bisquert, J.; Snaith, H. J.; Nicholas, R. J. Low-Temperature Processed Electron Collection Layers of Graphene/TiO_2 Nanocomposites in Thin Film Perovskite Solar Cells. *Nano Lett.* **2014**, *14*, 724−730.

(9) Wojciechowski, K.; Saliba, M.; Leijtens, T.; Abate, A.; Snaith, H. Sub-150 °C Processed Meso-Superstructured Perovskite Solar Cells with Enhanced Efficiency. *Energy Environ. Sci.* **2014**, *7*, 1142−1147.

(10) Abu Laban, W.; Etgar, L. Depleted Hole Conductor-Free Lead Halide Iodide Heterojunction Solar Cells. *Energy Environ. Sci.* **2013**, *6*, 3249−3253.

(11) Etgar, L.; Gao, P.; Xue, Z.; Peng, Q.; Chandiran, A. K.; Liu, B.; Nazeeruddin, M. K.; Grätzel, M. Mesoscopic $CH_3NH_3PbI_3/TiO_2$ Heterojunction Solar Cells. *J. Am. Chem. Soc.* **2012**, *134*, 17396−17399.

(12) Jeon, N. J.; Lee, J.; Noh, J. H.; Nazeeruddin, M. K.; Grätzel, M.; Seok, S. I. Efficient Inorganic−Organic Hybrid Perovskite Solar Cells Based on Pyrene Arylamine Derivatives as Hole-Transporting Materials. *J. Am. Chem. Soc.* **2013**, *135*, 19087−19090.

(13) Padovani, F. A.; Stratton, R. Field and Thermionic-Field Emission in Schottky Barriers. *Solid-State Electron.* **1966**, *9*, 695−707.

(14) Crowell, R.; Rideout, V. L. Normalized Thermionic-Field (T−F) Emission in Metal−Semiconductor (Schottky) Barriers. *Solid-State Electron.* **1969**, *12*, 89−105.

(15) Niu, G.; Li, W.; Meng, F.; Wang, L.; Dong, H.; Qiu, Y. Study on the Stability of $CH_3NH_3PbI_3$ Films and the Effect of Post-modification by Aluminum Oxide in All-Solid-State Hybrid Solar Cells. *J. Mater. Chem. A* **2014**, *2*, 705−710.

(16) Shi, J.; Dong, W.; Xu, Y.; Li, C.; Lv, S.; Zhu, L.; Dong, J.; Luo, Y.; Li, D.; Meng, Q.; Chen, Q. Enhanced Performance in Perovskite Organic Lead Iodide Heterojunction Solar Cells with Metal−Insulator−Semiconductor Back Contact. *Chin. Phys. Lett.* **2013**, *30*, 128402−128402.

(17) Ritala, M.; Leskela, M. Atomic Layer Epitaxy-A Valuable Tool for Nanotechnology? *Nanotechnology* **1999**, *10*, 19−24.

(18) Kusano, H.; Hosaka, S.; Shiraishi, N.; Kawakami, S.; Sugioka, K.; Kitagawa, M.; Ichino, K.; Kobayashi, H. Multi-Color Emission of PVCz-Based Multi-Layered Electroluminescent Devices. *Synth. Met.* **1997**, *91*, 337−339.

(19) Toshihide, Y.; Masakazu, N.; Yasuyuki, K. Palladium-Catalyzed Synthesis of Triarylamines from Aryl Halides and Diarylamines. *Tetrahedron Lett.* **1998**, *39*, 2367−2370.

(20) Im, J. H.; Lee, C. R.; Lee, J. W.; Park, S. W.; Park, N. G. 6.5% Efficient Perovskite Quantum-Dot-Sensitized Solar Cell. *Nanoscale* **2011**, *3*, 4088−4093.

(21) Lee, M. M.; Teuscher, J.; Miyasaka, T.; Murakami, T. N.; Snaith, H. J. Efficient Hybrid Solar Cells Based on Meso-Superstructured Organometal Halide Perovskites. *Science* **2012**, *338*, 643−647.

(22) Li, D.; Wang, M.; Wu, J.; Zhang, Q.; Luo, Y.; Yu, Z.; Meng, Q.; Wu, Z. Application of a New Cyclic Guanidinium Ionic Liquid on Dye-Sensitized Solar Cells (DSCs). *Langmuir* **2009**, *25*, 4808−4814.

(23) Liang, K. N.; Mitzi, D. B.; Prikas, M. T. Synthesis and Characterization of Organic−Inorganic Perovskite Thin Films Prepared Using a Versatile Two-Step Dipping Technique. *Chem. Mater.* **1998**, *10*, 403−411.

(24) Bi, D.; Moon, S. J.; Haggman, L.; Boschloo, G.; Yang, L.; Johansson, E. M. J.; Nazeeruddin, M. K.; Grätzel, M.; Hagfeldt, A. Using a Two-Step Deposition Technique to Prepare Perovskite ($CH_3NH_3PbI_3$) for Thin Film Solar Cells Based on ZrO_2 and TiO_2 Mesostructures. *RSC Adv.* **2013**, *3*, 18762−18766.

(25) Hegedus, S. S.; Shafarman, W. N. Thin-Film Solar Cells: Device Measurements and Analysis. *Prog. Photovoltaics* **2004**, *12*, 155−176.

(26) Guo, X. Z.; Luo, Y. H.; Zhang, Y. D.; Huang, X. C.; Li, D. M.; Meng, Q. B. Study on the Effect of Measuring Methods on Incident Photon-to-Electron Conversion Efficiency of Dye-Sensitized Solar Cells by Home-Made Setup. *Rev. Sci. Instrum.* **2010**, 81.

(27) Halaoui, L. I.; Abrams, N. M.; Mallouk, T. E. Increasing the Conversion Efficiency of Dye-Sensitized TiO_2 Photoelectrochemical Cells by Coupling to Photonic Crystals. *J. Phys. Chem. B* **2005**, *109*, 6334−6342.

(28) Garcia-Belmonte, G.; Boix, P. P.; Bisquert, J.; Sessolo, M.; Bolink, H. J. Simultaneous Determination of Carrier Lifetime and Electron Density-of-States in P_3HT:PCBM Organic Solar Cells under Illumination by Impedance Spectroscopy. *Sol. Energy Mater. Sol. Cells* **2010**, *94*, 366−375.
(29) Fabregat-Santiago, F.; Bisquert, J.; Cevey, L.; Chen, P.; Wang, M.; Zakeeruddin, S. M.; Grätzel, M. Electron Transport and Recombination in Solid-State Dye Solar Cell with Spiro-OMeTAD as Hole Conductor. *J. Am. Chem. Soc.* **2009**, *131*, 558−562.
(30) Fabregat-Santiago, F.; Bisquert, J.; Palomares, E.; Otero, L.; Kuang, D.; Zakeeruddin, S. M.; Grätzel, M. Correlation between Photovoltaic Performance and Impedance Spectroscopy of Dye-Sensitized Solar Cells Based on Ionic Liquids. *J. Phys. Chem. C* **2007**, *111*, 6550−6560.
(31) Garcia-Belmonte, G.; Munar, A.; Barea, E. M.; Bisquert, J.; Ugarte, I.; Pacios, R. Charge Carrier Mobility and Lifetime of Organic Bulk Heterojunctions Analyzed by Impedance Spectroscopy. *Org. Electron.* **2008**, *9*, 847−851.
(32) Fabregat-Santiago, F.; Garcia-Belmonte, G.; Mora-Sero, I.; Bisquert, J. Characterization of Nanostructured Hybrid and Organic Solar Cells by Impedance Spectroscopy. *Phys. Chem. Chem. Phys.* **2011**, *13*, 9083−9118.
(33) Kim, H. S.; Lee, J. W.; Yantara, N.; Boix, P. P.; Kulkarni, S. A.; Mhaisalkar, S.; Grätzel, M.; Park, N. G. High Efficiency Solid-State Sensitized Solar Cell-Based on Submicrometer Rutile TiO_2 Nanorod and $CH_3NH_3PbI_3$ Perovskite Sensitizer. *Nano Lett.* **2013**, *13*, 2412−2417.
(34) Qi, B.; Wang, J. Fill Factor in Organic Solar Cells. *Phys. Chem. Chem. Phys.* **2013**, *15*, 8972−8982.
(35) Rand, B. P.; Li, J.; Xue, J. G.; Holmes, R. J.; Thompson, M. E.; Forrest, S. R. Organic Double-Heterostructure Photovoltaic Cells Employing Thick Tris(acetylacetonato)ruthenium(III) Exciton-Blocking Layers. *Adv. Mater.* **2005**, *17*, 2714−2718.